Effect of Core-Corona Plasma Structure on Seeding of Instabilities in Wire Array *Z* Pinches

S. V. Lebedev, F. N. Beg, S. N. Bland, J. P. Chittenden, A. E. Dangor, M. G. Haines, S. A. Pikuz,* and T. A. Shelkovenko*
The Blackett Laboratory, Imperial College, London, SW7 2BZ, United Kingdom
(Received 1 March 2000)

We present the first measurements by x-ray radiography of the development of instabilities during the implosion phase of wire array *Z* pinches. The seeding of perturbations on the dense core of each wire is provided by nonuniform sweeping of the low-density coronal plasma from the cores by the global $\mathbf{J} \times \mathbf{B}$ force. The spatial scale of these perturbations ($\sim$0.5 mm for Al and $\sim$0.25 mm for W) is determined by the size of the wire cores ($\sim$0.25 mm for Al and $\sim$0.1 mm for W). A qualitative change in implosion dynamics, with transition to 0D-like trajectory, was observed in Al arrays when the ratio of interwire gap to wire core size was decreased to $\sim$3.

PACS numbers: 52.55.Ez

The spectacular progress in *Z*-pinch implosions of cylindrical wire arrays has resulted in the most powerful laboratory sources of soft x-ray radiation (280 TW, 4 ns, 1.8 MJ), relevant to inertial confinement fusion and other high energy density applications [1–4]. It is thought that the power and the rise time of the generated x-ray pulses are primarily determined by the development of the Rayleigh-Taylor (RT) instability in the imploding plasma. Reducing the amplitude of this instability can potentially lead to substantial increases in the maximum x-ray power, which can be achieved in wire array implosions. However, the initial conditions for the RT growth and the mechanism responsible for generating seed perturbations are not known. 2D magnetohydrodynamic (MHD) computational modeling (in r-z plane) [5] can successfully reproduce the x-ray pulse generated at stagnation of the plasma, but only by artificially adjusting the level of a purely random density perturbation. The initial plasma formation phase of wire array experiments, with discrete wires in a cylindrical array, is, however, intrinsically three dimensional. Both experimental data [6–9] and cold-start simulations [10,11] show that plasmas formed from the individual wires have heterogeneous structures with small dense cores, surrounded by low density coronal plasmas. In a wire array the global magnetic field produces a net radially inward $\mathbf{J} \times \mathbf{B}$ force, which blows the coronal plasma from the wires to the array axis and strongly affects the rate of ablation of the wire cores [12,13]. The growth of MHD instabilities in the plasma around each wire results in axial nonuniformity of this core ablation and provides the most likely mechanism for seeding mass perturbations in wire arrays.

In this Letter we present the first measurements by x-ray backlighting of the core plasma structures and the development of instabilities there in the run-in phase of wire array *Z*-pinch implosions. Comparison of these x-ray radiography data with simultaneously performed laser probing of the corona shows that instabilities, which are first seen in a low density coronal plasma around each wire, produce an imprint at the same wavelength ($\sim$0.5 mm for Al) on the dense wire cores when the array starts to implode. These imprinted perturbations provide a seed for subsequent development of a global $m = 0$ mode of the RT instability with a longer wavelength ($\sim$2 mm) [14]. A qualitative change in the implosion trajectory of wire cores (transition to 0D-like) was observed in Al arrays when the interwire gap decreased from 1.57 to 0.78 mm, the latter being 3 times greater than the measured size of Al wire core.

Experiments were performed on the MAGPIE generator [15] with current rising to 1 MA in 240 ns. Wire arrays 16 mm in diameter and 2.3 cm long were made of 8, 16, 32, and 64 wires (Al, 15 μm, W, 4 μm). The diagnostic setup included laser probing, soft x-ray gated camera, optical streak camera, and photoconducting detectors (PCDs) and is described elsewhere [9]. Point-projection x-ray radiography (Fig. 1) with high spatial ($<$15 μm) and temporal ($\sim$1 ns) resolution was performed using an *X* pinch [16], which was installed in one of the four return current conductors (77.5 mm from the array axis). The timing of the backlighting pulse was adjusted by the use of different wire diameters (20–50 μm Al) and different numbers of wires (2 or 4) in the *X* pinch. The energy of the probing radiation $h\nu \sim 3$–5 keV was determined by the emission spectrum of the *X* pinch [16] and by the transmission of the filter

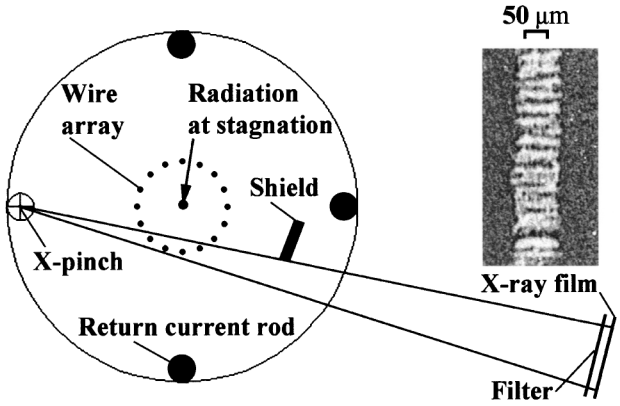

FIG. 1. Scheme of the experimental setup and radiographic image of 20 μm Ti wire in 16 wire array at 180 ns.

 0031-9007/00/85(1)/98(4)$15.00

(Ti, 12.5 μm) in front of the Kodak DEF film used for recording.

Figure 2 shows typical radiographic images of wires at the array edge obtained at ~70% of the implosion time and the corresponding radial profiles of the optical density. From these data the characteristic sizes of the wire cores are ~0.25 mm for Al and ~0.1 mm for W. These sizes are found to be the same for arrays with 16 and 64 wires, i.e., insensitive to the current in each wire. It is seen from Fig. 2 that the expansion of the wire cores for both materials is not symmetric in the inward and outward radial directions of the array, with a sharper boundary on the outer radius. A slower falloff in the inward radial direction indicates streaming of wire material to the array axis. The uniformity of wire cores on small spatial scales (comparable with the initial wire diameter) is different for different materials, similar to that observed in single wire Z-pinch explosions [7]. For example, Ti wires show a highly developed structure (Fig. 1) with a typical spatial scale of 10–20 μm, while no small-scale structure is seen in Al wire cores. At a longer spatial scale the axial distribution of mass averaged over 0.2–0.5 mm is fairly uniform at this early time for both Al and W.

The laser probing data show that low density coronal plasma formed around the wires expands much faster than the wire cores. At about half of the implosion time it arrives at the array axis and forms a precursor plasma column [9]. The expansion of the coronal plasma from the wires occurs with the development of instabilities (Fig. 3),

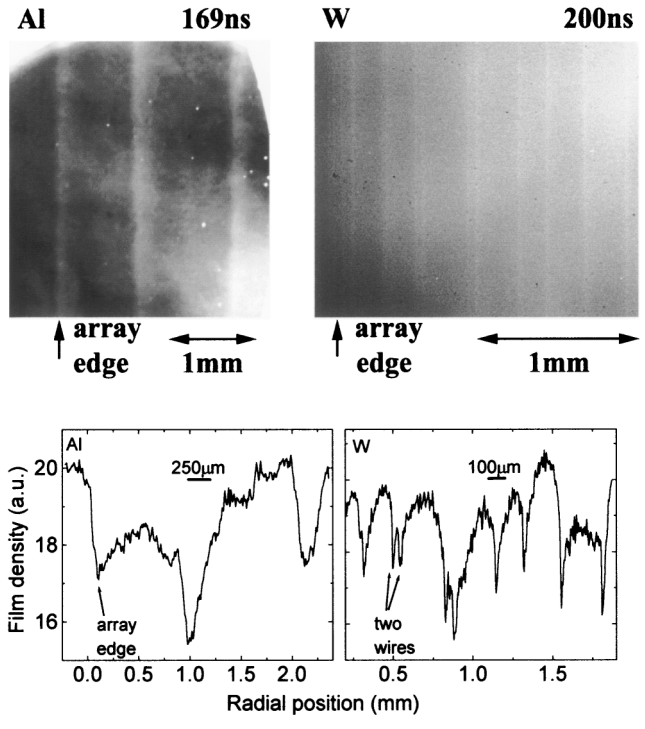

FIG. 2. Radiographic images of edge wires in Al and W arrays (above) and the corresponding radial profiles of film optical density (below).

which are seen from ~60 ns (~30% of implosion time) on schlieren and shadow images [9,14]. In contrast to single wire Z pinches (see, e.g., [6,17]), the instability pattern around each wire is not axially symmetric. This is due to the $\mathbf{J} \times \mathbf{B}$ force of the global B_θ magnetic field of the array, sweeping the coronal plasma to the axis. Another significant difference from a single wire Z pinch is a quasiperiodic structure of the instability, seen in the streams of the coronal plasma from each wire. The wavelength (λ) of this structure ($\lambda \sim 0.5$ mm for Al) does not change with time from 60 ns (when first seen) to ~200 ns, when the wire cores start to move from their initial positions, and is roughly constant in all wires. However, as reported earlier [14], there is no obvious correlation between the axial positions of the instability maxima and minima in different wires. The structure of the instabilities in the coronal plasma for other wire materials is similar to that observed for Al, but the wavelengths are different, ~0.4 mm for Ti and ~0.25 mm for W. There is no change in wavelength of the instability for different interwire separations between 6.3 and 0.78 mm (for 8–64 wires) and for different initial wire diameters (15, 20, 25 μm for Al and 4, 5, 7.5 μm for W).

The wavelength of the instability seen in the coronal plasma is comparable to the size of wire cores measured by x-ray radiography. Quantitative comparison can be performed by calculating the value of $ka = (2\pi/\lambda)a$, where λ is taken from the laser probing and the characteristic radius a is half of the core size (from radiography). The calculated ka (~1.6 and ~1.3 for, respectively, Al and W) are almost the same. This implies that the size of the region (~core size), where formation and acceleration of the coronal plasma take place, determines the development of the instability. The large extent of the instability structure in the inward radial direction [$\delta R \sim (5-10)\lambda$, Fig. 3] indicates a force-free character of these plasma streams

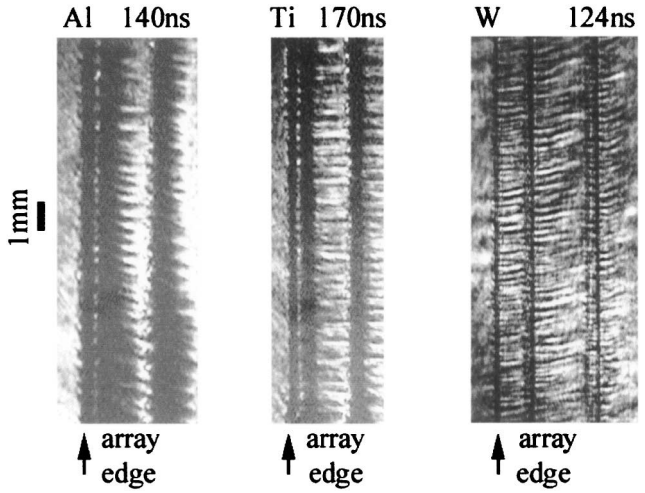

FIG. 3. Laser probing showing periodic structures in the coronal plasma for Al, Ti, and W wire arrays.

inside the array. A constant (in time) wavelength suggests that the size of the region where the coronal plasma is generated does not change significantly, which is also in agreement with the radiographic data in the time interval of 140–200 ns.

The observed axial nonuniformity of formation and sweeping of the coronal plasma from the wires should leave an imprint on the axial mass distribution in the wire cores. This may act as a seed for the development of RT instability during the acceleration of wires. Indeed, from ~80% of the implosion time, perturbations in wire cores start to be seen on the radiographic images. In Fig. 4, obtained for an aluminum wire array, it is seen that the outer boundary of the wires (the array edge) is nonuniform with a characteristic spikes and bubbles structure, which indicates development of RT instability in each individual wire of the array. The profiles of the film density along the wires [Fig. 4(b)] clearly show ~0.5 mm wavelength, the same as seen in the coronal plasma from early time. Wavelengths of instabilities measured on the different wires in Fig. 4 are the same, but the axial positions of spikes and bubbles in different wires generally do not coincide. These perturbations in individual wire cores act as a seed for the global $m = 0$ mode of RT instability, which develops later during further acceleration of the array [14]. However, this global mode at this later time has a longer wavelength ($\lambda \sim 2$ mm). The mechanism, which determines the wavelength of the correlated global mode in this three-dimensional system, requires further study but is probably related to the uncorrelated structure of perturbations in different wires. The $m = 0$ modes of the magneto RT instability have the fastest growth rates, but the different random axial positions of spikes and bubbles in different wires prevent the development of a global $m = 0$ mode with the same wavelength as that seen in individual wires. For a longer wavelength mode the effect of the perturbations being out of phase is smaller. Some indication of the preferential development of a longer wavelength structure (transition from 0.5 to ~2 mm) is seen in Fig. 4, where the amplitude (contrast) of perturbations is larger if axial positions of perturbations in neighboring wires coincide. It should be emphasized that the measurements presented here were obtained for arrays with interwire gaps of ~1.5–3 mm. The question of whether correlation of inhomogeneities in wire cores will appear for smaller gaps requires further investigation, e.g., radiographic measurements of wire cores in positions close to the array center, where shadows of the neighboring wires are not overlapping, which was not possible in the present experimental setup (Fig. 1).

The implosion dynamics of wire cores was measured by radial optical streak photography. It is instructive to compare these data (Fig. 5) with a 0D implosion model, which assumes that the array implodes as a hollow plasma cylinder accelerated by the global $\mathbf{J} \times \mathbf{B}$ force. The stagnation times measured from optical streaks and x-ray signals for arrays with different wire number agree to within <5% with implosion times calculated from the 0D model, as routinely observed in wire array Z-pinch implosions (see, e.g., [18]). However, the implosion trajectory for small wire number arrays deviates significantly from that predicted by the 0D model. For 8, 16, and 32 wire arrays the cores remain in their initial positions until about 80% of the implosion time (Fig. 5). This time coincides with the time when the imprint of instabilities on wire cores is detected by radiography. The stationary position of the wires can be understood only if no force is applied to the wire cores until this time; i.e., the current until this time flows mainly in the low density coronal plasma just around the wires. The sudden acceleration of the cores would then occur at the time of current transfer to the cores. For arrays with different wire number the current per wire at the time when the wires start to move varies by a factor of ~7 (Table I) and is definitely not a primary parameter here. The relative times of acceleration ($t_{ac}/t_{imp} \sim 0.8$), however, are the same for 8, 16, and 32 Al wire arrays and for 16, 32, and 64 tungsten wire arrays (Fig. 5), despite a very large difference in the thermal and ionization properties of Al and W. Assuming that all the current is transferred to

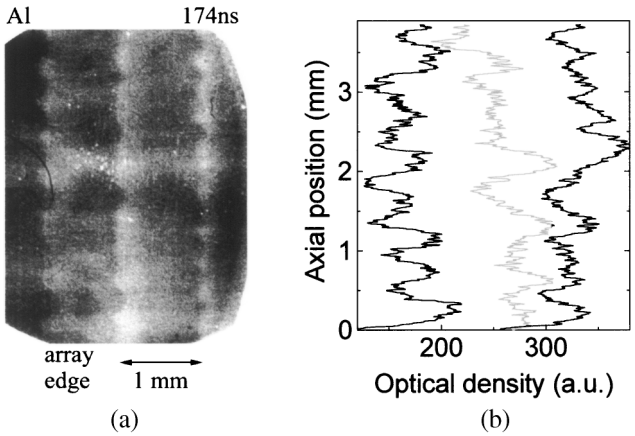

FIG. 4. Radiographic image showing instabilities in cores of Al wire array and corresponding axial profiles of film optical density (averaged over 0.2 mm).

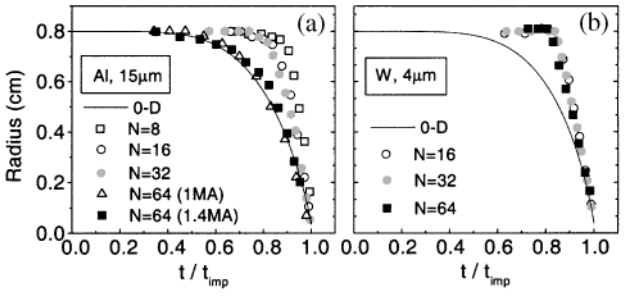

FIG. 5. Implosion trajectories measured from optical streaks for 8, 16, 32, and 64 Al (15 μm) wire arrays (a), and for 16, 32, and 64 W (4 μm) wire arrays (b). Time is normalized on the implosion time.

TABLE I. Times of the wires' acceleration (t_{ac}) and corresponding current (I_{ac}—total, I_{ac}/N—per wire) for arrays with different wire number. t_{imp} is the implosion time of the array.

N	I_{max} (MA)	t_{imp} (ns)	t_{ac} (ns)	t_{ac}/t_{imp}	I_{ac} (MA)	I_{ac}/N (kA/wire)
8 Al	1	200	168	0.84	0.76	95
16 Al	1	230	180	0.79	0.82	51
32 Al	1	270	208	0.77	0.95	30
64 Al	1	320	175	0.54	0.79	12
64 Al	1.4	270	145	0.53	0.85	13
16 W	1	200	165	0.83	0.75	47
32 W	1	230	190	0.83	0.87	27
64 W	1	270	220	0.82	0.97	15

the wire cores at the moment of ~80% of implosion time, a mass fraction of ~25%–50% remaining in the cores would provide the observed fast implosion.

A qualitative change in the implosion dynamics was observed in Al arrays when the wire number increases from 32 to 64 (interwire gap decreases from 1.57 to 0.78 mm). The measured array radius [Fig. 5(a)] for 64 wires follows the 0D trajectory very closely, and the inward displacement of wires from their initial radius occurs earlier (even in absolute time) than for a 32 wire array, despite a smaller (by a factor of 2) current per wire. The decrease of the interwire separation also changes the inward streaming of the coronal plasma at late time. This is evident from an early decay of the precursor emission, which is generated by stagnation of the coronal plasma streams on the array axis. This decay of precursor emission is seen on optical streaks, soft x-ray images (see Fig. 4 in Ref. [14]), and PCD signals, and for 64 wire array the precursor emission is not seen after about 200 ns, while for 32 and smaller wire number arrays the emission lasts until stagnation.

The observed qualitative change in the implosion dynamics (for Al wire arrays) occurred when the ratio between interwire separation (0.78 mm) and the characteristic size of wire core (0.25 mm) became equal to about 3. This could be related to the fact that when the ratio of the interwire separation to the wire diameter equals π, the contribution of the "private" magnetic flux of each wire to the array inductance [19] is zero, and the array inductance becomes equal to the inductance of a thin shell.

For tungsten wire arrays, which have a core size a factor of ~2.5 smaller, the transition to a 0D implosion trajectory for 64 tungsten wire array was not observed [Fig. 5(b)], and, unlike for aluminum, emission from the precursor continued until stagnation. This implies the absence of effective merger of plasmas from adjacent wires and instead a continuous injection of material from wire cores. Assuming that for the merger the same ratio of the gap to the size of wire core is necessary for both Al and W, a gap of <0.3 mm would be required to see this transition in tungsten wire arrays.

Our conclusion is that the development of perturbations in wire array Z pinches is dominated by the persistence of core-corona structure of plasma, formed from the wires. Seeding of perturbations on the wire cores is provided by the nonuniform formation and sweeping of the low density coronal plasma from the dense wire cores by the global $\mathbf{J} \times \mathbf{B}$ force. The size of wire cores determines the spatial scale of these nonuniformities, which are imprinted on dense wire cores and determine subsequent development of the RT instability. A qualitative change in the implosion dynamics, transition to 0D implosion trajectory of wire cores, was observed in Al wire arrays when the interwire separation was decreased to 0.78 mm, which is 3 times the size of the wire core. It is interesting to note that a dramatic change in the power versus gap dependence, observed in experiments with Al arrays on the 7 MA Saturn facility at Sandia National Laboratories (SNL) (Fig. 4 in Ref. [1]), occurred at about the same interwire gap (~1 mm). Smaller core size in tungsten wire arrays (~0.1 mm instead of ~0.25 mm for Al) explains the absence of transition to 0D implosion trajectory in our experiments and suggests that similar deviation of the implosion from 0D probably occurs in tungsten wire array experiments at SNL even for large wire number arrays.

The authors gratefully acknowledge useful discussions with Dr. A. L. Velikovich of the Naval Research Laboratory and Professor D. A. Hammer of Cornell University. This work was supported by Sandia National Laboratory (Grant No. BF-6405) and the U.S. DOE under Contract No. DE-FG03-98DP00217.

*Permanent address: P. N. Lebedev Physical Institute, Moscow, Russia.

[1] T. W. L. Sanford *et al.*, Phys. Rev. Lett. **77**, 5063 (1996).
[2] M. K. Matzen, Phys. Plasmas **4**, 1519 (1997).
[3] C. Deeney *et al.*, Phys. Rev. E **56**, 5945 (1997).
[4] R. B. Spielman *et al.*, Phys. Plasmas **5**, 2105 (1998).
[5] D. L. Peterson *et al.*, Phys. Plasmas **6**, 2178 (1999).
[6] D. Kalantar and D. Hammer, Phys. Rev. Lett. **71**, 3806 (1993).
[7] S. A. Pikuz *et al.*, Phys. Rev. Lett. **83**, 4313 (1999).
[8] C. Deeney *et al.*, Rev. Sci. Instrum. **68**, 653 (1997).
[9] S. V. Lebedev *et al.*, Phys. Plasmas **6**, 2016 (1999).
[10] J. P. Chittenden *et al.*, Phys. Rev. E **61**, 4370 (2000).
[11] I. R. Lindemuth *et al.*, Phys. Rev. Lett. **65**, 179 (1990).
[12] J. H. Hammer and D. D. Ryutov, Phys. Plasmas **6**, 3302 (1999).
[13] J. P. Chittenden *et al.*, Phys. Rev. Lett. **83**, 100 (1999).
[14] S. V. Lebedev *et al.*, Phys. Rev. Lett. **81**, 4152 (1998).
[15] I. H. Mitchell *et al.*, Rev. Sci. Instrum. **67**, 1533 (1996).
[16] T. A. Shelkovenko *et al.*, Rev. Sci. Instrum. **70**, 667 (1999).
[17] J. Ruiz-Camacho *et al.*, Phys. Plasmas **6**, 2579 (1999).
[18] T. W. L. Sanford *et al.*, Phys. Plasmas **5**, 3737 (1998).
[19] J. Katzenstein, J. Appl. Phys. **52**, 676 (1981).